

# Contents

<b>1</b>	<b>Introduction and Theory Overview</b>	<b>1</b>
1.1	Introduction . . . . .	1
1.2	Theory Overview . . . . .	2
1.2.1	Heavy Vector Triplet Model . . . . .	2
1.2.2	Basic Phenomenology . . . . .	3
1.2.3	Explicit Models . . . . .	8

# List of Figures

1-1	Branching ratios as a function of the resonan mass for the HVT bench- mark model A(left) and model B(right). . . . .	9
-----	---	---

# List of Tables

# Chapter 1

## Introduction and Theory Overview

### 1.1 Introduction

This thesis presents the analysis details and the results of the search for heavy resonances decaying into a  $Z$  boson and a Higgs boson ( $h$ ) at the center-of-mass energy of 8 TeV, using  $19.7\text{ fb}^{-1}$  p-p collision data. In turn, the  $Z$  boson is identified through its leptonic decays (Leptons often refer to  $e$  and  $\mu$  only in experiments.  $l = e, \mu$ ). The Higgs boson  $h$  is expected to hadronically decay into a pair of b-quarks. The investigated final states consist of two charged leptons which are identified in the detector and limit the presence of the background, and two b-quarks from the hadronic Higgs decay which collects the largest possible fraction of Higgs events.

This thesis is organised as follows. In the latter part of this chapter, the heavy resonances model is introduced, including the expected cross section and the specification of model parameters. In chapter 2, the LHC and the CMS experiment are introduced, including the information of each sub-detector and the trigger system of the CMS. The details of the analysis are shown in chapter 3. This chapter reveals the way to reconstruct physical objects in CMS. By adding some proper kinematic selections on those physics objects, the interested event in data collected by the CMS detector can be selected. Moreover, this chapter shows the comparison between data and simulation. In the last chapter, the results of the search and the conclusion are shown.

## 1.2 Theory Overview

Although the Higgs boson discovery by the ATLAS and CMS collaborations [1–3] imposes strong constraints on theories beyond the Standard Model(SM), the extreme fine tuning in quantum corrections required to have a light fundamental Higgs boson with mass close to 125 GeV [4–7] suggests that the Standard Model may be incomplete, and not valid beyond a scale of a few TeV. Various dynamical electroweak symmetry breaking scenarios which attempt to solve this naturalness problem, such as Minimal Walking Technicolor [8], Little Higgs [9–11], or compositeHiggs models [12–14] predict the existence of new resonances decaying to a vector boson plus a Higgs boson.

### 1.2.1 Heavy Vector Triplet Model

Resonant searches are typically not sensitive to all the details and the free parameters of the underlying model, but only to those parameters or combinations of parameters that control the mass of the resonance and the interactions involved in its production and decay. Therefore one can employ a simplified description of the resonance defined by a phenomenological Lagrangian where only the relevant couplings and mass parameters are retained. This model-independent strategy applies a Heavy Vector Triplet (HVT) [15] to the Standard Model group and reproduces a large class of explicit models. In Eq. (1.1), the mathematical form of the simplified Lagrangian is defined, where  $V_\nu^a$ ,  $a = 1, 2, 3$ , is a real vector with vanishing hypercharge in the adjoint representation of  $SU(2)_L$ , it describes one charged and one neutral heavy spin-1 particle with charge eigenstate fields, and  $D_{[\mu}V_{\nu]}^a$  represents the covariant derivative.

$$\begin{aligned} \mathcal{L}_V = & -\frac{1}{4}D_{[\mu}V_{\nu]}^a D^{[\mu}V^{\nu]a} + \frac{m_V^2}{2}V_\mu^a V^{\mu a} \\ & + ig_V c_H V_\mu^a H^\dagger \tau^a \overleftrightarrow{D}^\mu H + \frac{g^2}{g_V} c_F V_\mu^a \sum_f \bar{f}_L \gamma^\mu \tau^a f_L \\ & + \frac{g_V}{2} c_{VVV} \epsilon_{abc} V_\mu^a V_\nu^b D^{[\mu}V^{\nu]c} + \text{quadrilinear terms} \end{aligned} \quad (1.1)$$

$$V_\mu^\pm = \frac{V_\mu^1 \mp iV_\mu^2}{\sqrt{2}}, \quad V_\mu^0 = V_\mu^3 \quad (1.2)$$

$$D_{[\mu}V_{\nu]}^a = D_\mu V_\nu^a - D_\nu V_\mu^a, \quad D_\mu V_\nu^a = \partial_\mu V_\nu^a + g\epsilon^{abc}W_\mu^b V_\nu^c \quad (1.3)$$

44

45 In these models, new heavy vector bosons ( $V^\pm, V^0$ ) that couple to the Higgs and SM  
 46 gauge bosons with the parameters  $g_V$  and  $c_H$  and to the fermions via the combina-  
 47 tion  $(g^2/g_V)c_F$ . The parameter  $g_V$  represents the strength of the new vector boson  
 48 interaction, while  $c_H$  and  $c_F$  represent the couplings to the Higgs and the fermions  
 49 respectively, and are expected to be of order unity in most models.

## 50 1.2.2 Basic Phenomenology

### 51 Masses and Mixings

After electro-weak symmetry breaking (EWSB), the only massless state is the photon which can be identified as the gauge field associated with the unbroken  $U(1)_{em}$ . The two other neutral mass eigenstates are the SM  $Z$  boson and one heavy vector of mass  $M_0$  which are obtained by diagonalizing the mass matrix of the  $(Z, V^0)$  system by a rotation with angle  $\theta_N$

$$\begin{pmatrix} Z \\ V^0 \end{pmatrix} \rightarrow \begin{pmatrix} \cos \theta_N & \sin \theta_N \\ -\sin \theta_N & \cos \theta_N \end{pmatrix} \begin{pmatrix} Z \\ V^0 \end{pmatrix}. \quad (1.4)$$

The mass matrix is

$$\mathcal{M}_N^2 = \begin{pmatrix} \hat{m}_Z^2 & c_H \xi \hat{m}_Z \hat{m}_V \\ c_H \xi \hat{m}_Z \hat{m}_V & \hat{m}_V^2 \end{pmatrix}, \quad \text{where} \quad \begin{cases} \hat{m}_Z = \frac{e\hat{v}}{2 \sin \theta_W \cos \theta_W} \\ \hat{m}_V^2 = m_V^2 + g_V^2 c_{VVHH} \hat{v}^2 \\ \xi = \frac{g_V \hat{v}}{2 \hat{m}_V} \end{cases} \quad (1.5)$$

In the above equations  $\hat{v}$  denotes the Vacuum Expectation Value (VEV) defined by  $\langle H^\dagger H \rangle = \hat{v}^2/2$ , and one should know the masses  $\hat{m}_Z$  and  $\hat{m}_V$  do not coincide with the physical  $Z$  boson and new resonance masses of this model, although they do in the approximations later. The mass eigenvalues and the rotation angles are easily obtained by inverting the relations

$$\begin{aligned} Tr[\mathcal{M}_N^2] &= \hat{m}_Z^2 + \hat{m}_V^2 = m_Z^2 + M_0^2 , \\ Det[\mathcal{M}_N^2] &= \hat{m}_Z^2 \hat{m}_V^2 (1 - c_H^2 \xi^2) = m_Z^2 M_0^2 , \\ \tan 2\theta_N &= \frac{2c_H \xi \hat{m}_Z \hat{m}_V}{\hat{m}_V^2 - \hat{m}_Z^2} . \end{aligned} \quad (1.6)$$

Notice that the tangent can be uniquely inverted because the angle  $\theta_N$  is in the range  $[-\pi/4, \pi/4]$  in the parameter region we will be interested in, where  $\hat{m}_Z < \hat{m}_V$ .

The situation is similar in the charged vector where the mass matrix of the  $(W^\pm, V^\pm)$  system reads

$$\mathcal{M}_C^2 = \begin{pmatrix} \hat{m}_W^2 & c_H \xi \hat{m}_W \hat{m}_V \\ c_H \xi \hat{m}_W \hat{m}_V & \hat{m}_V^2 \end{pmatrix} , \text{ where } \hat{m}_W = \frac{e\hat{v}}{2 \sin \theta_W} = \cos \theta_W \hat{m}_Z , \quad (1.7)$$

and it is diagonalized by

$$\begin{aligned} Tr[\mathcal{M}_C^2] &= \hat{m}_W^2 + \hat{m}_V^2 = m_W^2 + M_\pm^2 , \\ Det[\mathcal{M}_C^2] &= \hat{m}_W^2 \hat{m}_V^2 (1 - c_H^2 \xi^2) = m_W^2 M_\pm^2 , \\ \tan 2\theta_C &= \frac{2c_H \xi \hat{m}_W \hat{m}_V}{\hat{m}_V^2 - \hat{m}_W^2} . \end{aligned} \quad (1.8)$$

By checking Eq. (1.5) and Eq. (1.7), the charged and neutral mass matrices are connected by custodial symmetry, which can be shown in full generality to imply

$$\mathcal{M}_C^2 = \begin{pmatrix} \cos \theta_W & 0 \\ 0 & 1 \end{pmatrix} \mathcal{M}_N^2 \begin{pmatrix} \cos \theta_W & 0 \\ 0 & 1 \end{pmatrix} . \quad (1.9)$$

By taking the determinant of the above equation, or equivalently by comparing the charged and neutral determinants in Eq. (1.6) and Eq. (1.8), we obtain a generalized custodial relation among the physical masses

$$m_W^2 M_\pm^2 = \cos^2 \theta_W m_Z^2 M_0^2 . \quad (1.10)$$

From the simple formula above, we can start to identify the physically reasonable region of the parameter space in this model. We aim at describing new vectors with masses at or above the TeV scale, but we also want the SM masses  $m_{W,Z} \sim 100$  GeV to be reproduced. Therefore we require a hierarchy in the mass relation of SM  $Z$  and  $W$  bosons versus the new vectors.

$$\frac{\hat{m}_{W,Z}}{\hat{m}_V} \sim \frac{m_{W,Z}}{M_{\pm,0}} \leq 10^{-1} \ll 1 \quad (1.11)$$

In the limit of Eq. (1.11) we obtain simple approximation for  $m_W$  and  $m_Z$

$$\begin{aligned} m_Z^2 &= \hat{m}_Z^2 (1 - c_H^2 \xi^2) (1 + \mathcal{O}(\hat{m}_Z^2 / \hat{m}_V^2)) , \\ m_W^2 &= \hat{m}_W^2 (1 - c_H^2 \xi^2) (1 + \mathcal{O}(\hat{m}_W^2 / \hat{m}_V^2)) . \end{aligned} \quad (1.12)$$

The parameter  $\xi$  can be either very small or of order unity. Both cases are realized in explicit models. While  $\xi \ll 1$  is the most common situation,  $\xi \sim 1$  only occurs in strongly coupled scenarios at very large  $g_V$ . In these approximations, SM tree-level experimental observation can be reproduced to percent accuracy.

Since  $\hat{m}_W = \cos \theta_W \hat{m}_Z$ , the  $W$ - $Z$  mass ratio is thus given by

$$\frac{m_W^2}{m_Z^2} \simeq \cos^2 \theta_W . \quad (1.13)$$

Eq. (1.13) has one important implication on the masses of the new vectors. When combined with the custodial relation Eq. (1.10), it tells us that the charged and



neutral  $V$ s are practically degenerate

$$M_{\pm}^2 = M_0^2(1 + \mathcal{O}(\%)) , \quad (1.14)$$

52 In the following, when working at the leading order in the limit Eq. (1.11), we can  
 53 ignore the mass splitting and denote the mass of the charged and the neutral states  
 54 collectively as  $M_V$ . It is easy to check that in that limit  $M_V = \hat{m}_V$ .

## 55 Decay Widths

Because of the hierachy in the mass matrices, the mixing angles are naturally small. By looking at Eqs. (1.6), (1.8) and (1.11) we can estimate

$$\theta_{N,C} \simeq c_H \xi \frac{\hat{m}_{W,Z}}{\hat{m}_V} \leq 10^{-1} , \quad (1.15)$$

and after rotating to the mass basis, the coupling of the neutral and charged resonances to left- and right-handed fermion chiralities can be written in a compact form for each fermion species  $F = \{l, q, 3\}$ .

$$\begin{cases} g_L^N = \frac{g^2}{g_V} \frac{c_F}{2} \cos \theta_C + (g_L^Z)_{SM} \sin \theta_N \simeq \frac{g^2}{g_V} \frac{c_F}{2} , \\ g_R^N = (g_R^Z)_{SM} \sin \theta_N \simeq 0 \\ g_L^C = \frac{g^2}{g_V} \frac{c_F}{2} \cos \theta_C + (g_L^W)_{SM} \sin \theta_C \simeq \frac{g^2}{g_V} \frac{c_F}{2} , \\ g_R^C = 0 \end{cases} \quad (1.16)$$

In the above equation  $(g_{L,R}^{W,Z})_{SM}$  denote the ordinary SM  $W$  and  $Z$  couplings (with the normalization given by  $g_L^W = g/\sqrt{2}$ ).

Given that the rotation angles are small, the couplings further simplify, as also shown in the equation. We could see that  $V$  interact mainly with left-handed chiralities and that all the couplings for each fermion species are controlled by the parameter

combination  $g^2/g_V c_F$ . This gives tight correlations among different channels

$$\Gamma_{V_{\pm} \rightarrow f \bar{f}'} \simeq 2\Gamma_{V_0 \rightarrow f \bar{f}'} \simeq N_C[f] \left( \frac{g^2 c_F}{g_V} \right)^2 \frac{M_V}{48\pi} , \quad (1.17)$$

where  $N_C[f]$  is the number of colors (3 for the di-quark and 1 for the dilepton decays). The parameters  $c_F = \{c_l, c_q, c_3\}$  control the relative BRs to leptons, light quarks and the third family.

In the case of di-boson decay width

$$\begin{aligned} \Gamma_{V_0 \rightarrow W_L^+ W_L^-} &\simeq \Gamma_{V_{\pm} \rightarrow W_L^{\pm} Z_L} \simeq \frac{g_V^2 c_H^2 M_V}{192\pi} \frac{(1 + c_H c_{VVV} \xi^2)^2}{(1 - c_H^2 \xi^2)^2} = \frac{g_V^2 c_H^2 M_V}{192\pi} [1 + \mathcal{O}(\xi^2)] , \\ \Gamma_{V_0 \rightarrow Z_L h} &\simeq \Gamma_{V_{\pm} \rightarrow W_L^{\pm} h} \simeq \frac{g_V^2 c_H^2 M_V}{192\pi} \frac{(1 - 4c_{VVHH} \xi^2)^2}{1 - c_H^2 \xi^2} = \frac{g_V^2 c_H^2 M_V}{192\pi} [1 + \mathcal{O}(\xi^2)] . \end{aligned} \quad (1.18)$$

56 Note that Eq. (1.18) is derived in the Equivalent Gauge [16] because the decay to  
 57 transverse SM vectors is highly suppressed while to the longitudinal parts grows with  
 58 the energy of the process, therefore the Unitary Gauge which is used in the original  
 59 Lagrangian is instead useful. The channels that are not shown in the above equations  
 60 are either forbidden, like  $hh$  and  $\gamma\gamma$  decays, or suppressed like the decays to transverse  
 61 polarizations.

62 From this section, a very simple picture emerges. At small  $\xi$ , all the decay widths  
 63 are fixed with a given resonance mass  $M_V$  and the couplings  $\{g^2 c_F/g_V, g_V c_H\}$  which  
 64 control the BRs in all relevant channels. Parameters  $c_{VVV}$ ,  $c_{VVHH}$  and  $c_{VW}$  are  
 65 basically irrelevant. Thus, the basic phenomenology of this model is well described  
 66 by a good approximation.

### 1.2.3 Explicit Models

Now the general picture is clear, we can get exact values of the widths and BRs from explicit models. Consider two benchmark models, A and B, which correspond to two explicit models describing the heavy vectors in Refs. [17] and [12] respectively. All the  $c$  parameters are fixed to specific values in these models and the only free parameters are the resonance mass  $M_V$  and coupling  $g_V$ . Moreover, model A is inspired by weakly coupled extensions of the SM gauge group while model B is by strongly coupled scenarios of EWSB, *i.e.* Composite Higgs models, we will consider them in different regions of  $g_V$ , relatively small  $g_V \leq 3$  and relatively large  $g_V \geq 3$ .

Figure 1-1 shows the BRs as functions of the mass in model A and B. As expected from the previous discussion and according to Refs. [17], model A predicts

$$\begin{aligned} c_H &= -g^2/g_V^2, \quad c_F \simeq 1, \\ |g_V c_H| &\simeq g^2 c_F / g_V \simeq g^2 / g_V. \end{aligned} \quad (1.19)$$

Therefore Eq. (1.17) and (1.18) can be determined in the following form for  $V_0$  in model A ( $g_V = 1$ ),

$$\begin{aligned} \Gamma_{V_0 \rightarrow f \bar{f}'} &\simeq N_c[f] \frac{g^4 M_V}{96\pi} \\ \Gamma_{V_0 \rightarrow W^+ W^-} &\simeq \Gamma_{V_0 \rightarrow Z h} \simeq \frac{g^4 M_V}{192\pi}. \end{aligned} \quad (1.20)$$

One can easily check either from the plot or the equation, a factor of two difference comparing the BRs between fermions and bosons. Due to the color factor, leptons and quarks also have a difference by a factor of three. Since the  $c_F$  term is universal both in A and B. The total width in model A decreases with increasing  $g_V$  because of the overall suppression ( $g^2/g_V$ ) in Eq. (1.19).

On the contrary, in model B the  $c_H$  term is unsuppressed

$$c_H \simeq c_F \simeq 1 ,$$

$$g_V c_H \simeq -g_V , g^2 c_{c_F} / g_{g_V} \simeq g^2 / g_V . \quad (1.21)$$

Thus the determinate  $V_0$  decay widths for model B ( $g_V = 3$ ) are

$$\Gamma_{V_0 \rightarrow f \bar{f}} \simeq N_c[f] \frac{g^4 M_V}{342\pi}$$

$$\Gamma_{V_0 \rightarrow W^+ W^-} \simeq \Gamma_{V_0 \rightarrow Zh} \simeq \frac{3M_V}{64\pi} . \quad (1.22)$$

68 For model  $B_{g_V=3}$  the dominant BRs are into di-bosons and the fermionic decays are  
 69 extremely suppressed. Moreover, the total width increases with increasing  $g_V$  since it  
 70 is dominated by the di-boson width which grows with  $g_V$  as expected from Eq. (1.21).  
 71 This model B is particularly interesting for the present search, since it predicts signal  
 72 cross sections in order of fb [15] [18], branching ratios to vector bosons close to unity,  
 73 and thus being accessible at the LHC. In the latter chapters, the mass eigenstate of  
 74 the neutral heavy vector boson in model B scenario refers to the  $Z'$  particle, which is  
 75 the search target of this thesis.

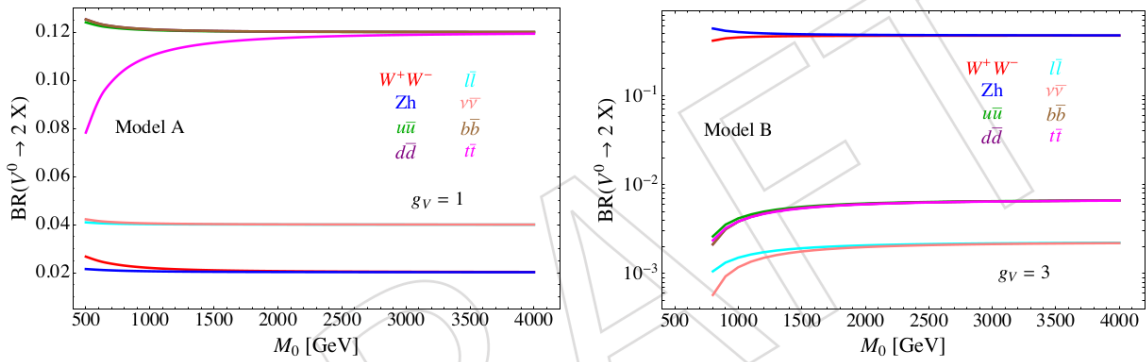


Figure 1-1: Branching ratios as a function of the resonant mass for the HVT benchmark model A(left) and model B(right).

# Bibliography

- [1] ATLAS Collaboration. Observation of a new particle in the search for the Standard Model Higgs boson with the ATLAS detector at the LHC. *Phy. Lett. B*, 716:1, 2012.
- [2] CMS Collaboration. Observation of a new boson at a mass of 125 GeV with the CMS experiment at the LHC. *Phy. Lett. B*, 716:30, 2012.
- [3] CMS Collaboration. Observation of a new boson with mass near 125 GeV in pp collisions at  $\sqrt{s} = 7$  and 8 TeV. *JHEP*, 06:081, 2013.
- [4] CMS Collaboration. Precise determination of the mass of the Higgs boson and tests of compatibility of its couplings with the standard model predictions using proton collisions at 7 and 8 TeV. *Eur. Phys. J. C*, 75:212, 2015.
- [5] ATLAS Collaboration. Measurement of the Higgs boson mass from the  $H \rightarrow \gamma\gamma$  and  $H \rightarrow ZZ^* \rightarrow 4l$  channels in pp collisions at center-of-mass energies of 7 and 8 TeV with the ATLAS detector. *Phys. Rev. D*, 90:052004, 2014.
- [6] ATLAS Collaboration. Evidence for the spin-0 nature of the Higgs boson using ATLAS data. *Phys. Lett. B*, 726:120, 2013.
- [7] CMS and ATLAS Collaboration. Combined Measurement of the Higgs Boson Mass in pp Collisions at  $\sqrt{s} = 7$  and 8 TeV with the ATLAS and CMS Experiments. *Phys. Rev. Lett.*, 114:191803, 2015.
- [8] Mads T. Frandsen. Minimal Walking Technicolor. arXiv:0710.4333 [hep-ph], <http://arxiv.org/abs/0710.4333>, 2007.
- [9] B. McElrath T. Han, H. E. Logan and L.-T. Wang. Phenomenology of the little Higgs model. *Phys. Rev. D*, 67:095004, 2003.
- [10] M. Schmaltz and D. Tucker-Smith. LITTLE HIGGS THEORIES. *Annual Review of Nuclear and Particle Science*, 55:no. 1, 229–270, 2005.
- [11] M. Perelstein. Little Higgs models and their phenomenolog. *Progress in Particle and Nuclear Physics*, 58:no. 1, 247–291, 2007.
- [12] D. Marzocca R. Contino, D. Pappadopulo and R. Rattazzi. On the effect of resonances in composite Higgs phenomenology. *Journal of High Energy Physics*, 2011:no. 10, 1–50, 2011.

- 107 [13] M. Serone D. Marzocca and J. Shu. General composite Higgs model. *Journal of*  
108 *High Energy Physics*, 2012:no. 8, 1–52, 2012.
- 109 [14] C. Cski B. Bellazzini and J. Serra. Composite Higgses. *Eur. Phys. J.*, C74:no.  
110 5, 2766, 2014.
- 111 [15] R. Torre D. Pappadopulo, A. Thamm and A. Wulzer. Heavy vector triplets:  
112 bridging theory and data. *Journal of High Energy Physics*, 2014:no. 9, 1–50,  
113 2014.
- 114 [16] Andrea Wulzer. An Equivalent Gauge and the Equivalence Theorem.  
115 arXiv:1309.6055 [hep-ph], <http://arxiv.org/abs/1309.6055>, 2013.
- 116 [17] W.-Y. Keung V. Barger and E. Ma. Gauge model with light W and Z bosons.  
117 *Phys. Rev. D*, 22:727, 1980.
- 118 [18] Lisa Benato, Yu-Hsiang Chang, Ching-Wei Chen, Michele de Gruttola, Ra-  
119 man Khurana Ji-Kong Huang, Stefano Lacaprara, Yun-Ju Lu, Jacopo Pazzini,  
120 Maurizio Pierini, Henry Yee-Shian Tong, Jun-Yi Wu, Shin-Shan Eiko Yu, Marco  
121 Zanetti, and Alberto Zucchetta. Search for heavy resonances decaying into a vec-  
122 tor boson and a higgs boson in the  $(ll, l\nu, \nu\nu)b\bar{b}$  final state. CMS Note 2015/186,  
123 CMS, 2015.